Theoretical Exploration of Josephson Plasma Emission in Intrinsic Josephson Junctions

Masashi Tachiki[a,d] and Masahiko Machida[b,c,d]

[a] National Research Institute for Metals, Sengen 1-2-1, Tsukuba, Ibaraki 305 Japan
[b] Argonne National Laboratory MSD Bldg.232, 9700 Cass Ave. Argonne, IL60439 US
[c] Japan Atomic Energy Research Institute, 2-2-54 Nakameguro, Meguroku, Tokyo 153-0061 Japan
[d] CREST, Japan Science and Technology Corporation(JST), Japan

ABSTRACT

In this paper, we theoretically predict the best efficient way for electromagnetic wave emission by Josephson plasma excitation in intrinsic Josephson junctions. First, we breifly derive basic equations describing dynamics of phase differences inside junction sites in intrinsic Josephson junctions, and review the nature of Josephson plasma excitation modes based on the equations. Especially, we make an attention to that Josephson plasma modes have much different dispersion relations depending on the propagating directions and their different modes can be recognized as N standing waves propagating along ab-plane in cases of finite stacked systems composed of N junctions. Second, we consider how to excite their modes and point out that excitations of in-phase mode with the highest propagation velocity among their N modes are the most efficient way for electromagnetic wave emissions. Finally, we clarify that in-phase excitations over all junctions are possible by using Josephson vortex flow states. We show simulation results of Josephson vortex flow states resonating with some Josephson plasma modes and predict that superradiance of electromagnetic field may occur in rectangular vortex flow state in which spatiotemporal oscillations of electromagntic fields are perfectly in-phase.

Keywords: intrinsic Josephson junction, Josephson plasma, electromagnetic wave emission, Josephson vortex, superradiance

1. INTRODUCTION

All High-Tc superconducting oxide materials have multi-layered crystal structures composed of strong superconducting layer CuO_2 and non-superconducting layer. Since this character is very important in considering applications of High-Tc cuprate superconductors, many investigations searching nature of layered superconductors have been prompted [1]. Many artificial multilayered materials basically show interesting rich behaviors depending on choices of stacking compounds and stacking methods. On the other hand, in High-Tc oxide materials, single crystal itself is a multi-layered system. This means that High-Tc oxide basically has a possiblity showing rich and applicapable material properties. Therefore, many investigations pursuing those properties have been performed and many curious natures connecting with layered structures have been revealed. In this paper, we focus on a group of High-Tc cuprates showing especially strong anisotropy among many High-Tc oxides. The reason is that highly anisotopic cuprate materials intrinsically show properties as multi-stack of Josephson junctions [2],[3]. In those materials, non-superconducting layers play a roll of insulating layer and a coupling between neighboring superconducting layers becomes well-known Josephson coupling via Cooper pair tunneling. Thus, single crystals of those materials have been called intrinsic Josephson junctions and expected to have peculiar and valuable properties opening new application fields of High-Tc cuprates [4].

In this paper, we suggest an effective application using intrinsic Josephson junctions. First, we show theoretical perspectives for the systems. They are intimately connected with recent intensive studies for Josephson plasma excitation [5]. It is well known that single Josephson junctions generally have an excitation mode confined inside its junction site. This mode is called Josephson plasma mode because it is originated from Coulomb interaction between Cooper pairs. Now, the following question must arise for intrinsic Josephson junctions. How is spectrum

Further author information: (Send correspondence to Masahiko.Machida)
Masashi Tachiki: E-mail: tachiki@crest.kkjj.crest.go.jp
Masahiko Machida: E-mail: machida@bernstein.msd.anl.gov, mac@koma.jaeri.go.jp

DISCLAIMER

DISCLAIMER

Portions of this document may be illegible in electronic image products. Images are produced from the best available original document.

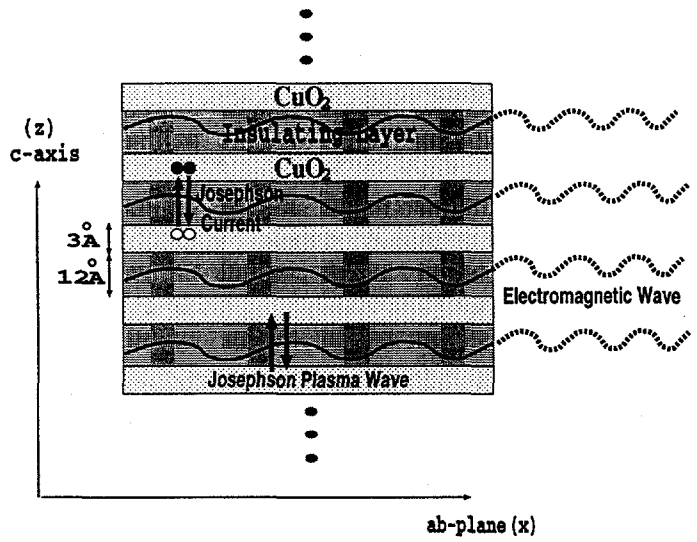

Figure 1. A schematic figure for intrinsic Josephson junctions. Electromagnetic waves are emitted by excitations of Josephson plasma.

of the excitation mode in intrinsic Josephson junctions different from that of the single junction ? This is because those systems are atomic-scale multi-stacked systems and the existence of collective excitations over all junctions can be expected. In fact, Tachiki, Koyama, and Takahashi et al. show that the excitation modes can be basically characterized by two kinds of modes, that is, transverse and longitudinal Josephson plasma modes [4]. Here, let us explain a differecce between the two modes. Since oscillating directions of all modes are fixed to c-axis, the modes can be distinguished by their propagating directions. The transverse mode means that its propagating direction is in ab-plane, while both oscillating and propagating directions are along c-axis in the longitudinal mode. Thus, the following characters with respect to the two collective modes have been clear. The transverse mode can be assigned as an electromagnetic wave propagating inside insulating medium, while the longitudinal mode is a new charge fluctuation mode and it can emerge only in atomic-scale stacked systems [6],[7],[8].

Next, let us consider about a new application using those peculiar natures of the collective modes. Though we have some ideas [4], we focus on only a subject which studies potentialities as generators of electromagnetic wave [9],[10],[11]. It is well known that Josephson junction systems generally show electromagnetic wave emissions in resistive states and its detection have been employed as a confirmation for AC Josephson effects [2]. This can be theoretically explained by Josephson relation connecting the time development of superconducting phase with appling DC Voltage and the sinusoidal dependence for the superconducting phase in expression of Josephson current. Actually, though the emissions have been detected in many experiments, the power was too weak to be widely employed as a generator. However, the use of Josepshon junctions has an advantage that frequency of emitted electromagnetic wave is controlable. Therefore, many attempts to improve emission power have been made and some experiments successfully enhanced the power [12]. Especially, experiments using junction array systems under the magnetic field show very remarkable results [12]. Generally, in multi-oscillator systems, a synchronization over many oscillators are the most important event. This is because it leads to drastic power enhancement and focusing of emitted wave frequency, that is, a laser amplification. Therefore, in this paper, we consider eletromagnetic emissions using this synchronization effect in intrinsic Josephson junctions as seen in schematic figure 1, where Josephson plasma waves in all junction sites are in-phase. Now, we may expect that many junctions of intrinsic Josephson junctions easily synchronize because the coupling between junctions is very strong due to atomic-scale stacked systems as shown in Fig.1 (note thickness of both superconducting and inslulating layers). This is a simple expectation, but we show that it is actually possible in this paper. In fact, numerical experiments by Machida et al. clearly show that synchronizations over all junctions occur by using flux flow dynamics [13]. Moreover, they clarified that the synchronization can be seen in a wide range of transport current or generated voltage [13].

Let us show the outline of this paper. In section II, we breifly review a theoretical background of Josephson plasma

modes in intrinsic Josephson junctions. We give dispersion relations of collective excitaitons and consider what is essential for efficient electromagnetic wave emissions. In section III, we show numerical simulation results for flux flow under the layer parallel magnetic field and c-axis parallel transport current, and clarify how fluxon dynamics interact with Josephson plasma modes and how electromagnetic waves emit from intrinsic Josephson junctions. Moreover, we discuss about possibilities of superradiance in flux flow states. Finally, we summarize our results and point out high possibilities as an excellent generator of electromagnetic wave.

2. THEORY OF COLLECTIVE EXCITATIONS

In this section, we review nature of collective excitations in intrinsic Josephson junctions. At first, we start with theoretical considerations for the system and derive an equation describing dynamics of the phase differences in all Josephson junctions . The collective excitation modes can be extracted by linearizing the equation.

Now, let us give a model for intrinsic Josephson junctions [14]. Fig.1 is a schematic view for the systems. It represents a simplified picture composed of two superconducting and insulating layers. Among cuprate layered superconductors, $La_{2-x}Sr_xCuO_4$(LSCO) has single CuO_2 plane, while $Bi_2Sr_2CaCu_2O_{8+y}$(BSSCO) has double CuO_2 planes. However, this difference is not essential in investigating nature as stacked Josephson junctions. This is because the coupling between double CuO_2 planes is so strong that the coupling is not related with low energy physics much below the superconducting gap energy. Thus, it is found that the simple model as seen in Fig.1 is valid enough for BSSCO. In addition, we assume that that spatial differences along c-axis for the superconducting phase and vector potential inside the superconducting layer can be neglected. As seen in Fig.1, even for cases with double layers thickness of superconducting layer is so thin ($\approx 3\mathring{A}$). Therefore, the superconducting phase can be assumed to vary only along the ab-plane and its variation is connected with the superfluid velocity along the ab-plane as $\mathbf{v}_\ell^{ab} = \frac{\hbar}{2m}(\nabla_{ab}\theta_\ell - \frac{\phi_0}{2\pi}\mathbf{A}_\ell^{ab})$, where ℓ means ℓ-th layer, θ_ℓ is the superconducting phase at ℓ-th layer, and vectors with suffix $_{ab}$ are ones defined in ab-plane. In inslulating layers, a link variable is defiend as a path integral variable along c-axis like, $(A^z_{\ell+1,\ell}) = \int_\ell^{\ell+1} A_z$, and a gauge invariant superconducting phase difference is defined as $\varphi_{\ell+1,\ell}(\equiv \theta_{\ell+1} - \theta_\ell - \frac{2\pi}{\phi_0}\int_\ell^{\ell+1} A_z)$. A total c-axis current is given by

$$j^z_{\ell+1,\ell} = j_c sin\varphi_{\ell+1,\ell} + \sigma_c E^z_{\ell+1,\ell} + \frac{\epsilon_c}{c}\frac{\partial E^z_{\ell+1,\ell}}{\partial t} \tag{1}$$

where σ_c and ϵ_c are the quasiparticle conductivity and the dielectric constant along the c-axis in the insulating layer, respectively. This expression represnts that c-axis current is composed of the Josephson, the quasi-particle, and the displacement currents. The dynamics of electormagnetic fields can be described by the Maxwell equation,

$$\frac{\epsilon_c}{c}\frac{\partial E^z_{\ell+1,\ell}}{\partial t} + \frac{4\pi}{c}(j_c sin\varphi_{\ell+1,\ell} + \sigma_c E^z_{\ell+1,\ell}) = \frac{\partial B^y_{\ell+1,\ell}}{\partial x}, \tag{2}$$

$$-(B^y_{\ell+1,\ell} - B^y_{\ell,\ell-1}) = s\frac{4\pi}{c} j^x_\ell, \tag{3}$$

$$E^z_{\ell+1,\ell} - E^z_{\ell,\ell-1} = \frac{4\pi s}{\epsilon_c}\rho_\ell, \tag{4}$$

where $E^z_{\ell+1,\ell}$ and $B^y_{\ell+1,\ell}$ are the electric field in z-axis and the magnetic field in y-axis, and those dyanmics are directly connected with low energy dynamics of phase difference $\varphi_{\ell+1,\ell}$. In the right hand side of eq.(3), the displacement current component is dropped since it is irrelevant with above low energy dynamics. Also, ρ_ℓ is the charge density at ℓ-th layer. Here, it should be noted that the magnetic field direction is fixed to be in y-direction. This is because fluctuations along vortex lines under the magnetic field can be almost neglected in low temperature range. Thus, it is enough to deal with $E^z_{\ell+1,\ell}$ and $B^y_{\ell+1,\ell}$ only. The Josephson relations describing Josephson effects are given as follows,

$$\frac{\partial \varphi_{\ell+1,\ell}}{\partial t} = \frac{2\pi c D}{\phi_0} E^z_{\ell+1,\ell}, \tag{5}$$

$$\frac{\partial \varphi_{\ell+1,\ell}}{\partial x} = \frac{8\pi^2\lambda^2_{ab}}{c\phi_0}(j^x_{\ell+1} - j^x_\ell) + \frac{2\pi D}{\phi_0} B^y_{\ell+1,\ell}. \tag{6}$$

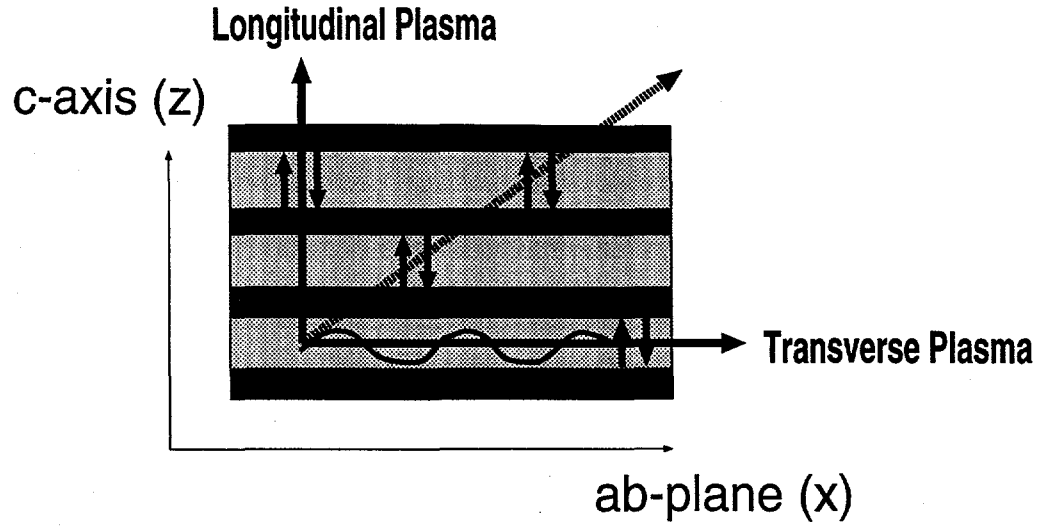

Figure 2. A schematic figure for propagations and oscillations of Josephson plasma modes. The long and short arrows indicate propagating and oscillating directions, respectively.

From those expressions, we can obtain a dynamical equation (called coupled Sine-Gordon equation) [13],[15] in terms of only the phase difference as follows,

$$\begin{aligned}\frac{\partial^2\varphi_{\ell+1,\ell}}{\partial t'^2} &= \frac{{\lambda_{ab}}^2}{sD}\left(\frac{\partial^2\varphi_{\ell+2,\ell+1}}{\partial t'^2}+\frac{\partial^2\varphi_{\ell,\ell-1}}{\partial t'^2}-2\frac{\partial^2\varphi_{\ell+1,\ell}}{\partial t'^2}\right)\\ &+ \frac{{\lambda_{ab}}^2}{sD}\left(sin\varphi_{\ell+2,\ell+1}+sin\varphi_{\ell,\ell-1}-2sin\varphi_{\ell+1,\ell}\right)\\ &+ \beta\frac{{\lambda_{ab}}^2}{sD}\left(\frac{\partial\varphi_{\ell+2,\ell+1}}{\partial t'}+\frac{\partial\varphi_{\ell,\ell-1}}{\partial t'}-2\frac{\partial\varphi_{\ell+1,\ell}}{\partial t'}\right)\\ &+ \frac{\partial^2\varphi_{\ell+1,\ell}}{\partial x'^2}-sin\varphi_{\ell+1,\ell}-\beta\frac{\partial\varphi_{\ell+1,\ell}}{\partial t'},\end{aligned} \tag{7}$$

where $t'=\omega_p t$ and $x'=x/\lambda_c$ with ω_p and λ_c being, respectively, the Josephson plasma frequency ($\omega_p=\frac{c}{\sqrt{\epsilon}\lambda_c}$) and the penetration depth in the c-axis direction. The parameter $\beta(\equiv\frac{4\pi\sigma\lambda_c}{\sqrt{\epsilon}c})$ is related to the McCumber parameter β_c as $\beta_c=1/\beta^2$. Here, let us consider tiny oscillation modes of the phase difference $\varphi_{\ell+1,\ell}$ on eq.(7). Since the system is basically two dimension, propagating directions of the modes have two degree of freedoms, which are c-axis (z) and ab-plane (x) directions as shown in Fig.2. Here, by noting that the oscillating direction is always fixed to be c-axis, collective modes can be recognized as mixtures of the two components which are longitudinal and transverse modes [4]. In other words, the modes propagating along general directions have both components of transverse and longitudinal modes. For the purpose of deriving dispersion relations for those modes, we neglect terms in terms of dissipation and linearize nonlinear terms in coupled Sine-Gordon equation (7). By inserting the plane wave solution propagating along ab-plane as, $\varphi_{\ell+1,\ell}=e^{ik_x x-i\omega t}f_{\ell+1,\ell}$ where $f_{\ell+1,\ell}=\sum_n g_n e^{\frac{i\pi\ell n}{N}}$, we can obtain the following dispersion relation [13],

$$\omega_p^{(n)}(k_x)=\omega_p\sqrt{1+k_x^2/[1+\frac{2\lambda_{ab}^2}{sD}(1-\cos\frac{n\pi}{N})]}, \tag{8}$$

where N is the number of stacked junctions and n varies from 0 to N-1. Here, note that periodic boundary conditions are applied for a system of N stacked junction. It is found that N modes exist in cases regarding N junctions as an unit of system. According to the relation, the dispersion relation of $\omega^{(n)}(k_x)$ with $n=0$ is the most dispersive, while $\omega^{(n)}(k_x)$ with $n=N-1$ shows an almost flat dispersion. The dipsersions of other modes assigned as $n=1$ to $n=N-2$ lie between those of the two modes $n=0$ and $n=N-1$. Now, let us consider what the mode label

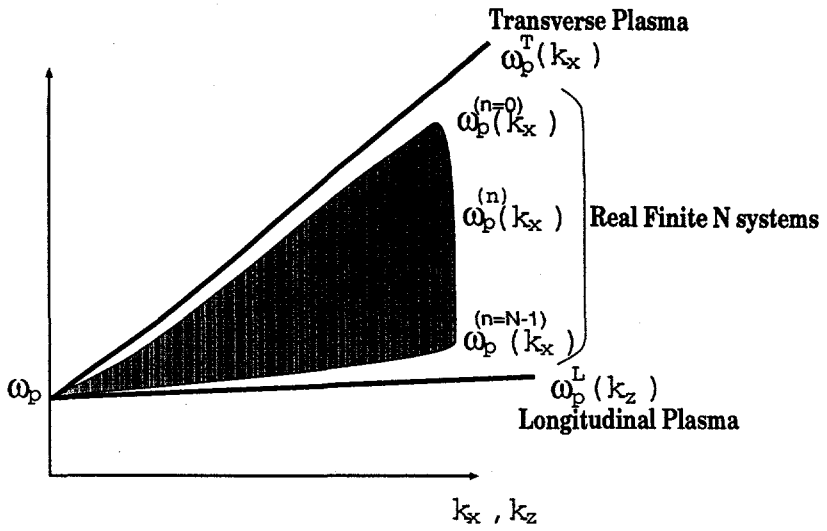

Figure 3. A schematic figure of dispersion relation of Josephson plasma modes in intrinsic Josephson junction. The dispersion relations in finite N junction systems are schematically depicted, and those of the transverse and longitudinal mode in infinite system are added.

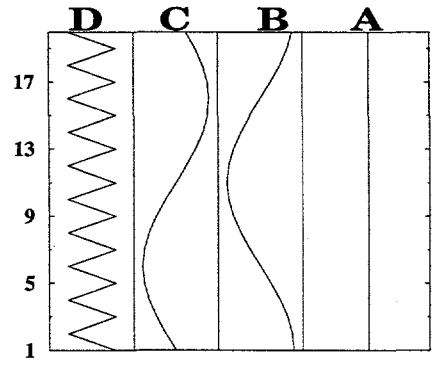

Figure 4. The variations of $f_{\ell+1,\ell}$ along c-axis of four modes (n=0,1,2,and 19) in a system with N=20. A,B,C, and D coreespond to n=0,1,2, and 19, respectively.

n means in real finite systems. As an example, we handle a case of $N = 20$ below. Here, we note that we impose a special condition on top and bottom junctions. This condition comes from real situations that top and bottom junctions can couple only with lower and upper junctions, respectively, and the dispersion relations are different from a case appling the periodic boundary condition. Those differences are schematically shown in Fig.3, where dispersion relations for finite N systems are located within a shaded region. Fig.4 shows four types among variations of $f_{\ell+1,\ell}$ along c-axis in a finite N=20 case. The type A(n=0) is perfectly in-phase mode along c-axis, while the type B(n=1), C(n=2), and D(n=19) have nodes along c-axis. The differences between those modes reflects phase shifts of plasma waves propagating in successive junctions. Fig.5 shows two examples in which phase shifts between neighboring junction sites are zero and finite. The lower figure shows a situation that propagating waves are perfectly in-phase over all junction sites, while in upper one those are out of phase.

Now, let us consider how phase shifts along c-axis affect emissions of electromagnetic waves from intrinsic Josephson junctions. The propagating plasma waves inside junction sites decompose into reflecting and outgoing waves at sample edge, and outgoing waves are converted into electromagnetic waves in vacuum space. The in-phase mode just correpsonds to parallel plasma waves propagating along ab-plane, and it has no components in the longitudinal

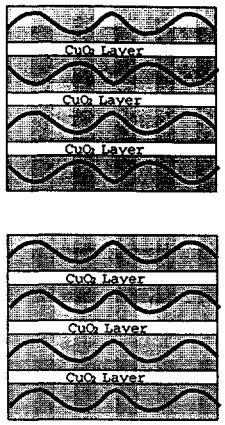

Figure 5. A schematic view of the propagating waves. The upper figure shows in-phase propagating waves, while the lower one shows those with phase shifts between neighboring junctions.

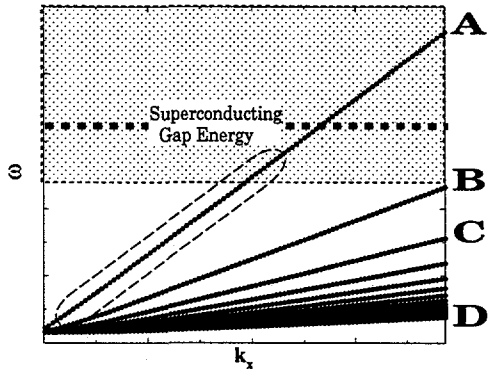

Figure 6. The excitaion spectrum of the Josephson plasma in N=20 stacked junction systems. A, B, C, and D stands for plasma waves with phase shifts along c-axis as seen in Fig.4, respectively. In the hatched region, damping effects are so strong that decay of excited plasma waves becomes remarkable.

direction. Therefore, the conversion processes to electromagnetic waves are dynamically parallel in all junctions and those do not cancel each other. On the other hand, propagating plasma waves with phase shifts along c-axis has standing wave components along c-axis, and those components cause cancelation among electromagnetic waves converted in edges of successive junctions. Thus, it is clear that excitations of the in-phase plasma mode are essential for applications as electromagnetic wave generators. Fig.6 shows excitation spectrum for finite stacked junction systems (N=20). From above considerations, the best way for efficient radiations is found to excite in-phase mode surrounded by a dashed line in Fig.6. In addition, it should be noted that there is an upper limit for frequency in the spectra of in-phase mode. This is because damping effects rapidly increase at frequencies near the superconducting gap energy. Thus, the problem becomes how we excite the in-phase plasma mode in an appropriate frequency region.

Up to now, many methods to excite plasma waves in intrinsic Josephson junctions have been suggested [4],[9],[10],[16]. For example, since the discovery of intrinsic Josephson junctions, Tachiki, Koyama, and Takahashi et al. proposed methods using AC Josephson effect [4] and flux flow [9],[10], while Shafranjuk and Tachiki studied excitations by quasi-particle injection [16]. However, those early works did not clear which kinds of modes are excited by their proposed methods, and overlooked syncronization effects between junctions. Therefore, we investigate the dynamics of the superconducting phase differences in all junction sites in more details and explore conditions in which synchronizations between junctions can occur [13]. Let us go back to the basic equation (eq.(7)) describing the dynamics of phase difference. The equation has two type excitations. One type is tiny oscillating plane wave solution as

mentioned above, and another type is a topological excitaiton which corresponds to Josephson vortex [17]. A vortex solution is basically a nonlinear solution and it can move like a soliton. However, the toplogical solution in the coupled Sine-Gordon equation (eq.(7)), certainly interacts with collective modes under its motion since the equation is not integrable compared to so-called Sine-Gordon equation. In other words, its motions cause ripple waves behind center of vortices [18]. In this paper, we show that many vortices interact each other via Josephson plasma waves and some resonant flux flow states appear [13]. Especially, we clarify that a resonant flow state with in-phase plasma mode can emerge [13]. For the purpose of simulating dynamics of both toplological and collective excitations, we perform numerical simulations for the coupled Sine-Gordon equation (eq.(7)) and show how flux flow states actually changes by resonating with collective modes [13].

3. NUMERICAL EXPERIMENTS FOR FLUX FLOW AND JOSEPHSON PLASMA EXCITAION

In this section, we briefly show numerical simulation techniques and reveal that flux flow states show rich varieties over a wide region of I-V characteristics. In order to characterize such various behaviors we classify flux flow states into four typical regions and investigate time developments of electric fields excited at the sample edge in each region. Thus, we discuss how electromagnetic wave emission occurs in those flux flow states, and predict which is the most efficient region for electromagnetic wave emission.

Now, let us turn to numerical simulations for flux flow states. Figure.7 is a schematic figure for systems to be simulated. The magnetic field and the transport current are applied along ab-plane (y-axis) and c-axis, respectively. Under such a condition, the magnetic flux penetrate as Josephson vortices and those move along ab-plane (-x-axis). The equation to be solved numerically to simulate such a situation is the coupled Sine-Gordon equation (eq.(7)) [14],[15]. The terms of the equation can be divided into two groups, one of which characterizes nature as single Josephson junction and another of which describes the coupling between neighboring junctions. The latter group has a coefficient $\frac{\lambda_{ab}^2}{sD}$ and the magnitude is very large in intrinsic Josephson junctions. This phisically means that vortex currents flow over many junctions since those systems are atomic scale junctions [19]. Therefore, it is found that correlations of phase differences between neighboring junctions are very strong under the presence of parallel magnetic field [19].

In numerical simulations for eq.(7), we set material parameters s, D, λ_{ab}, and $\beta(\equiv \frac{4\pi\sigma\lambda_c}{\sqrt{\epsilon}c})$ to be $3\mathring{A}$, $12\mathring{A}$, $0.25\mu m$, and 0.1. Though the value of β has some ambiguities by depending on the sample, it is shown by numerical simulations that qualitative features, i.e., appearing resonant vortex flow states are almost equivalent. Generally, when β is decreased, all resonances happen at lower current values. This is clearly because vortex speed can become higher under the same transport current when the dissipation is weak (β is small). In other words, the changes of β just shift resonant points. In addition, λ_c and $\omega_p(\equiv \frac{c}{\sqrt{\epsilon}\lambda_c})$ employed as units for rescaling time and length are set to be $125\mu m$ and $480GHz$, and anisotropic parameter γ is set to be 500(it is automatically determined by λ_{ab} and λ_c). In this paper, we report numerical simulation data for a finite size IJJ composed of 20 junctions (N=20). The simulation region is the ac cross section (the xz-plane in Fig.8) which is 2-dimensional (2D) rectangular shape. The transport current and the magnetic field including the self-field induced by transport current are, respectively, introduced through the boundary conditions at the top and bottom layers and the edges of all the layers. To perform the simulations we divide the region ($L \times N$) into 400 meshes along the x-direction and take 20 junctions along c-axis. In addition, each mesh width along x-axis is $0.1\lambda_{ab}$. Thus, the system size used in the simulations corresponds to an area of $10\mu m \times 20$ junctions and is comparable to a typical experimental size using $Bi_2Sr_2CaCu_2O_8$. We consider only cases in which all junctions sites are filled up by vortices enough. Therefore, the applied magnetic field reported in this paper is fixed to be 2T. Simulation results in lower field than 1T are qualitatively different. Those results will be published elsewhere [20]. The results shown below are qualitatively size-independent. We confirmed this fact by performing the simulations for system sizes up to $30\mu m \times 80$ junctions in real scale.

Now, let us show simulation results. Figure 9 is I-V characteristics. It is found that there are three step like structures as shown by arrow in the figure. By monitoring all flux flow states by visualizing the phase differences in all junctions, we can find that flux lattice flow structures drastically changes at those step like structures. Thus, flux flow states can be divided into four regions. It is also found that each flux flow state is almost a steady state inside each region by monitoring of $\varphi_{\ell+1,\ell}$. Let us see typical steady flux flow states inside four regions. Figure 10(I) is a snapshot of flux flow states in region I. In the figure, phase differences $\varphi_{\ell+1,\ell}$ of all junction sites and positions of vortex center are described together. As seen in Fig.10(I), any types of vortex lattice configurations can not be

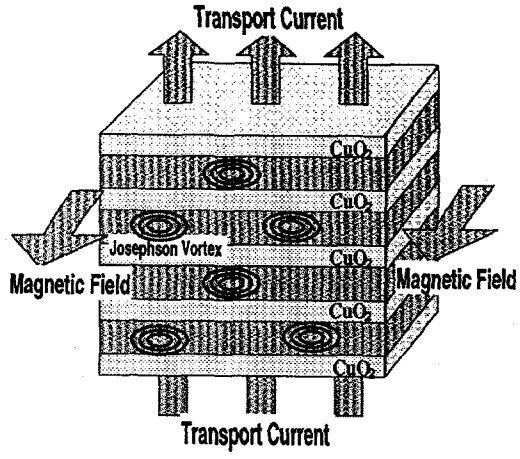

Figure 7. A schematic figure of flux flow states simulated numerically. The magnetic field and the transport current are applied along ab-plane and c-axis, respectively.

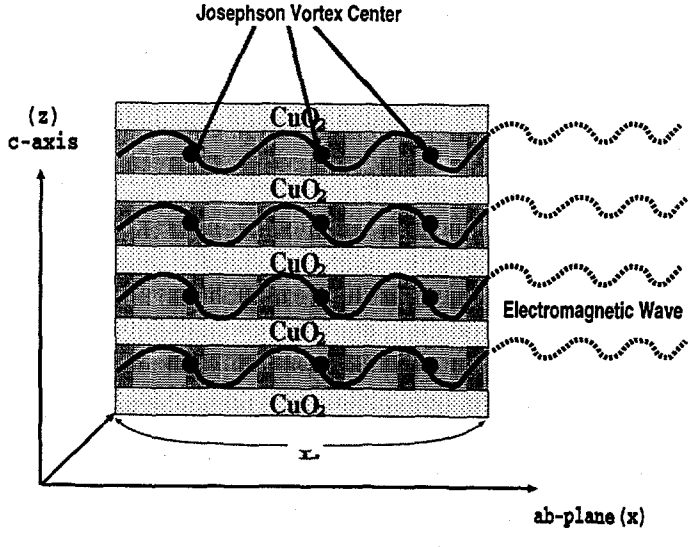

Figure 8. A schematic view of a vortex flow state resonated with the in-phase plasma mode. The circles indicate centers of vortices. The real curves inside junction sites stand for variations of phase differences, while the dashed curves outside the junctions correspond to electromagnetic waves converted at edges.

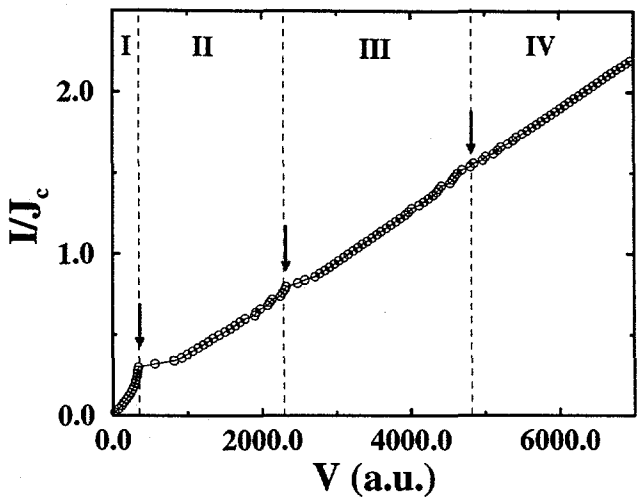

Figure 9. The simulated I-V characteristics. Three step like structures are observed as shown by downward arrows, and I-V characteristics are divided into four regions.

observed and vortex motions are almost chaotic. In this region I, currents flow inhomogeniously and its inhomogenity breaks vortex lattice correlation. We found that open boundary condition at sample surfaces has an essential roll on their chaotic motions. This is because triangular vortex flow states are stable in region I for simulations employing periodic boundary conditions on x-axis. Thus, we can expect that such chaotic motions appear in experimental situations using samples with open edges along ab-plane. The simulation results for periodic boundary condition in which sample edge effects are removed will be published elsewhere [20]. Let us see flux flow states in region II. The region appears after the most clear step like structure is observed with increasing the current. In region II, it is found that some correlations along c-axis develop as seen in Fig.10(II). This is because resonances between vortex flow and some plasma modes occur. Figure 11 show the simulated I-V characteristics where the vertical lines correspond to voltages satisfing the conditions as $k_x = H = 2T$ and $w_p = V$ in dispersion relations (Fig.6). Generally, resonances with eigen modes give rise to drastic enhancements of amplitude of resonant modes. Therefore, the resonant modes in the present system develop, and flux flow states themselves seem to adjust propagating shapes of the resonant modes. Let us show flux flow states of region III in Fig.10(III). In this region, fluxons are found to align completely along c-axis and a perfect rectangular lattice appears. In addition, such a rectangular lattice is found to be stable over all regime inside region III. This is because vortex correlation along c-axis more strongly develops by a resonance with mode B as seen in Fig.11. However, we have a following question. Though we have a theoretical expectation that flux flow state adjusting the mode B should be a node along c-axis, simulation results show a perfect vortex alignment along c-axis. The reason may be explained as follows, First, we have to point out that mode analysis can predict only some resonant points with linear modes. At those resonant points drastic changes of states happen but nonlinearity has an important roll in regions deviated from resonant points. It means that there may be coupling with modes over wide regions of excitation spectrum due to nonlinearity. Thus, resonances with the mode A may occur in region III prior to a resonant point predicted by the linear analysis. However, such an answer is not theoretically enough, and more refined analysis including nonlinear effects are required [11]. Next, let us see flux flow states in region IV after a resonance with the highest mode A. In this region, triangular like lattice flow states emerge as seen in Fig.10(IV). If a resonance with the mode A occurs, we can anticipate that flux flow state should adjust the shape of mode A. However, the results show behaviors as if an instability for the mode occurs. This fact may be explained as below. In region IV, the fluxons move with higher speed than mode A with the highest speed. This means that flux motions can not resonate with any collective modes in this region. Therefore, flux motions in this state are determined only by a balance of dissipation and driving force induced by the transport current. As a result, it is considered that standard flow state, that is, triangular like lattice emerges.

Next, let us consider how electromagnetic wave emissions occurs in each region. As seen in a schematic Fig.8,

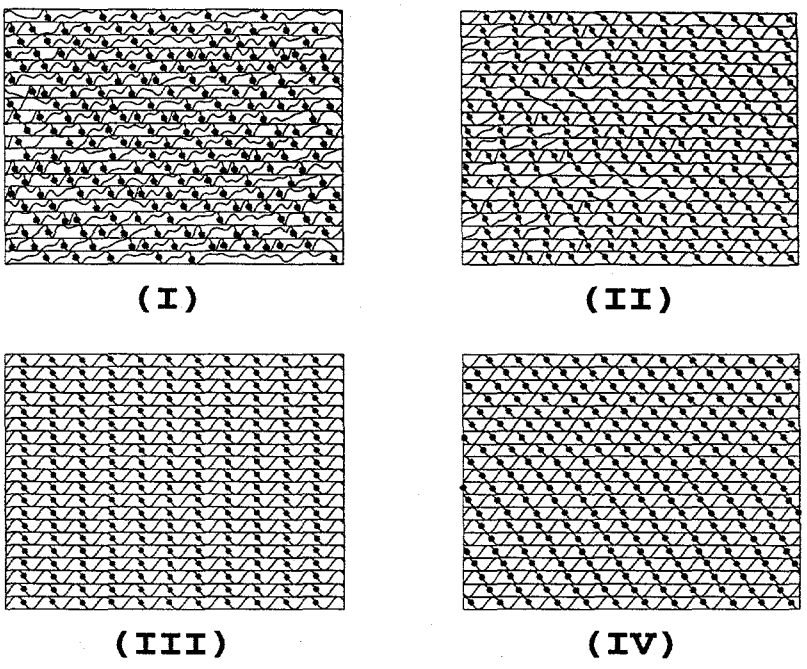

Figure 10. Snapshots of flux flow states from region I to region IV. Each figure shows a typical steady state which can be observed in corresponding region of I-V characteristics.

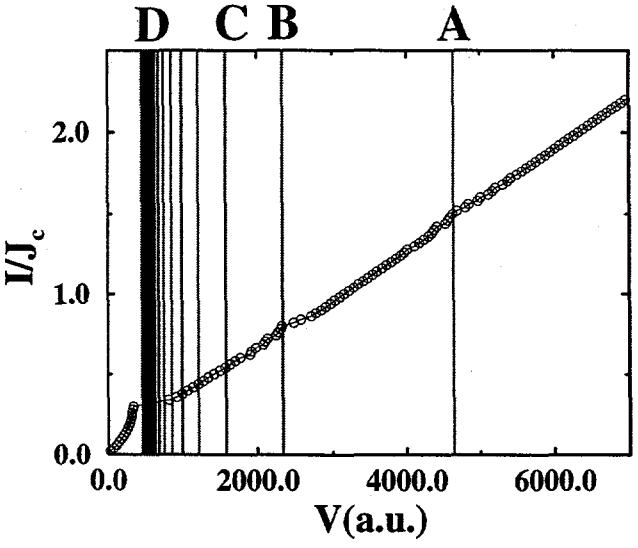

Figure 11. I-V characteristics same as the Fig.9. The vertical lines represent resonant voltages with plasma waves, and A, B, C, and D correspond to resonant voltages with modes seen in Fig.4 and 6, respectively. The resonant conditions are $\omega_p^{(n)} = V$ under $k_x = H = 2T$.

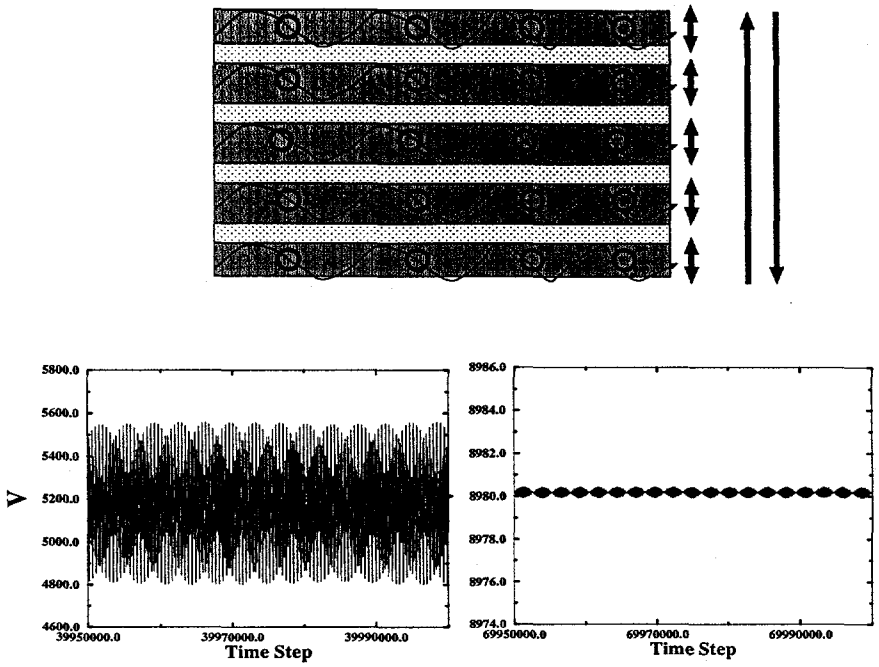

Figure 12. Upper panel: a schematic figure for electric field oscillations at junction edges in flux flow states. Lower panel: time developments of total electric fields at the sample edge $\sum_\ell E_{\ell+1,\ell}(t, x = L)$ in region III and IV. The left and right hand side correspond to $\sum_\ell E_{\ell+1,\ell}(t, x = L)$ in region III and IV, respectively.

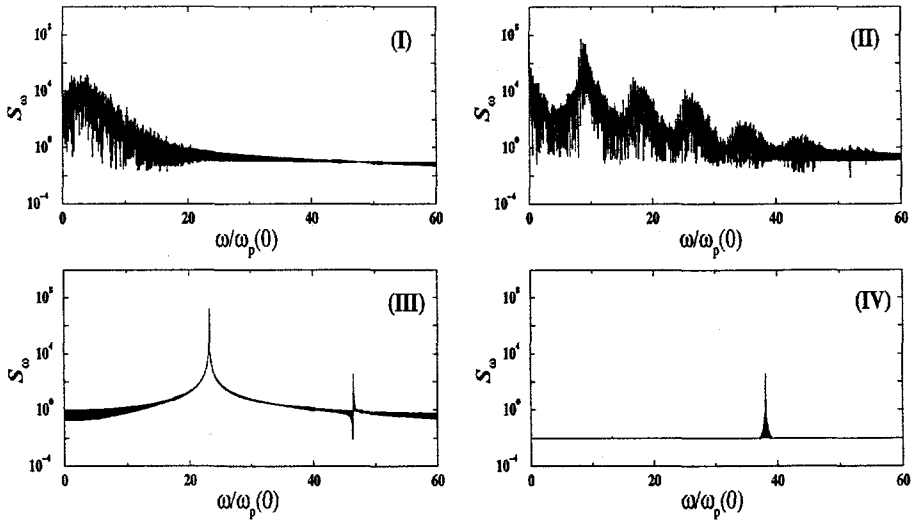

Figure 13. The power spectrum of $\sum_\ell E_{\ell+1,\ell}(x = L, t)$ observed in each region. The number at upper right hand side of each figure corresponds the region number as seen in Fig.9.

vortex motions give rise to oscillation components with DC electric field in each junction site. This AC components propagate through junction sites, while a part of those is converted into electromagnetic wave at sample edge. The behaviors are considered to be similar to a radiation of electromagnetic wave by dipole moment oscillation. This is because the electric field at each junction edge oscillates as seen in the upper panel of Fig.12. Now, what is the most important conditions for strong emission of electromagnetic wave in this system ? It is to realize a state in which oscillations at successive junction edges do not cancel each other. If electric field oscillations at edges of all junctions are in-phase, the magnitude of a dipole moment increases in proportion to the number of junctions as seen in the upper panel of Fig.12 . As an example, let us see differences between electric field oscillations at sample edge in the region III and IV. The lower panels in Fig.12 shows time developments of total sum of electric fields at right edges ($\sum_\ell E_{\ell+1,\ell}(x = L)$) in region III and IV. The figure at the left hand side corresponds to data measured in region III and clearly shows that large oscillation components exist, while the figure at the right hand side means that electric fields at edges almost cancel in region IV. Thus, it is found that the power of emission like dipole radiation is drastically enhanced in the region III. Let us study power spectrum for time developments of $\sum_\ell E_{\ell+1,\ell}(x = L)$ in each region. It is considered that the power spectrum reflect structures of spectrum of emitted electromagnetic waves. Figure 13 (I),(II),(III), and (IV) are typical power spectrum observed in each region, respectively [13]. In region I, power spectrum are broad and show f^{-2} dependence in high frequency region since flux motions are chaotic. Since the alignment of vortices along c-axis develop in the region II and region III, those power spectrum show peak structures at a frequency and its higher harmonics. This is because a distance between neighboring vortices along x-axis in each junction site is almost fixed and therefore time variation of electric fields becomes almost periodic. Especially, it should be noted that the peak structure in region III is extremely sharp and the power at the peak position is very large. Thus, it is found that very strong emission in a fixed frequency is possible in region III. In addition, it is found that though peak structures in region IV are very sharp the power at the peak frequency is much smaller than region III. In the region, though vortex lattice correlation develop well and the distance between neighboring vortices is alsmot a constant, electric field oscillations between neighboring junctions are almost canceled. Thus, though spectrum is sharp, the power becomes very low.

4. SUMMARY AND CONCLUSION

In this paper, we reviewed that collective excitaiton modes in intrinsic Josephson junctions have wide varieties by differences of those propagating directions. The number of those modes is the same as the number of junctions in finite stacked systems, and those modes can be distinguished by shapes of modulations along the c-axis of propagation waves. We emphasized that excitations of an in-phase mode among many modes are the most important and show that its excitation is possible by using flux flow states. By performing numberical simulation for the coupled Sine-Gordon equation, we clarified that flux flow states change their lattice flow structures by resonances with collective modes and in-phase rectangular lattice flow states emerge. In Josephson vortex flow states, we found that electric field at sample edges behaves like oscillating dipole moment, and electromagnetic wave emissions like dipole radiation may happen. The moment becomes very large in proportion to the number of stacked junctions in rectangular lattice flow state, while it is strongly depressed by cancelation between successive junctions in triangular like lattice flow state. Thus, we can conclude that experimental realization of rectangular lattice flow state is the most important condition and superradiation of electromagnetic waves is possible only in the state due to synchronization over all junctions. We believe that studies exploring such a state lead to realization of excellent electromagnetic wave generators, that is, Josephson plasma laser in the future.

5. ACKNOWLEDGMENTS

The authors thank T.Yamashita for useful discussions. M.Machida thanks A.E.Koshelev for helpful discussions. This work was completed in Argonne National Laboratory. The authors thank staff members of superconductivity and magnetism group in Argonne National Laboratory.

REFERENCES

1. G. Blatter, M.V.Feigel'man, V.B.Geshkenbein, A.I.Larkin, and V.M.Vinokur, "Vortices in High-temperature Superconductors" *Rev.Mod.Phys.* **66**, pp.1125, 1994.
2. R. Kleiner, F.Steinmeyer, G.Kunkel, and P.Müller, "Intrinsic Josephson Effects in $Bi_2Sr_2CaCu_2O_{8+y}$ Syngle Crystals" *Phys.Rev.Lett.* **68**, pp.2394–2397, 1992.

3. G. Oya, N.Aoyama, A.Irie, S.Kishida, and H.Tokutaka, "Observation of Josephson Junction Like Behaviors in Single Crystal (Bi, Pb)$_2$Sr$_2$CaCu$_2$O$_y$" *Jpn. J. Appl. Phys.* **31**, pp.L829–L831, 1992.
4. M. Tachiki, T.Koyama, and S.Takahashi, "Electromagnetic Phenomena Related to a Low Frequency Plasma in Cuprate Superconductors" *Phys. Rev.* **B 50**, pp.7065–7084, 1994.
5. Y. Matsuda, M. B. Gaifullin, K. Kumagai, K. Kadowaki, and T. Mochiku, " Collective Josephson plasma resonance in the vortex state of $Bi_2Sr_2CaCu_2O_{8+y}$" *Phys.Rev.Lett.* **75**, pp.4512–4515, 1995.
6. T.Koyama and M.Tachiki, "I-V characteristics of Josephson-coupled layered superconductors with longitudinal plasma excitations" *Phys. Rev.* **B 54**, pp.16183–16191, 1996.
7. M.Machida, T.Koyama, and M.Tachiki, "Instability of Longitudinal Plasma Oscillations and Intrinsic AC Josephson Effects in Josephson Coupled High-Tc Superconductors", *Physica* **C300**, pp.55–58, 1998.
8. M.Machida, T.Koyama, and M.Tachiki, "Dynamical Breaking of Charge Neutrality in Intrinsic Josephson Junctions: Common Origin for Microwave Resonant Absorptions and Multiple-Branch Structures in the I-V Characteristics", *Phys.Rev.Lett.* **83**, pp.4618–4621, 1999.
9. T.Koyama and M.Tachiki, "Plasma Excitation by Flux Flow" *Sol.St.Comm.* **96**, pp.367–371, 1995.
10. M.Machida, T.Koyama, S.Takahashi, and M.Tachiki, "Direct Numerical Simulations on Superconducting Plasma Excitation by Flux Flow in Layered High-Tc Superconductors" *Physica* **C293**, pp.87–91, 1997.
11. A.E.Koshelev and A.I.Aranson, "Dynamic Structure Selection and Instabilities of Driven Josephson Lattice in High-Temperature Superconductors" (Preprint).
12. P.Barbara, A.B.Cawthorne, S.V.Shitov, and C.J.Lobb, "Stimulated Emission and Amplification in Josephson Junction Arrays" *Phys.Rev.Lett.* **82**, pp.1963–1966, 1999.
13. M.Machida, T.Koyama, A.Tanaka, and M.Tachiki, "Collective Dynamics of Josephson Vortices in Intrinsic Josephson Junctions: Exploration of In-phase Locked Superradiant Vortex Flow States " *Physica* **C330**, pp.85–93, 2000
14. M.Machida, T.Koyama, A.Tanaka, and M.Tachiki, "Theory of the Superconducting Phase and Charge Dynamics in Intrinsic Josephson-junction Systems: Microscopic Foundation for Longitudinal Josephson Plasma and Phenomenological Dynamical Equations " *Physica* **C331**, pp85–96, 2000
15. L.N.Bulaevskii, M.Zamora, D.Baeriswyl, H.Beck, and J.R.Clem, "Time-dependent equations for phase differences and a collective mode in Josephson-coupled layered superconductors" *Phys.Rev.* **50**, pp.12831–12833 ,1994
16. S.E.Shafranjuk and M.Tachiki, " Emission of plasmons caused by quasiparticle injection to a high-Tc superconductor" *Phys.Rev.* **59**, pp.14087–14091, 1999.
17. J.R.Clem and M.W.Coffey, "Viscous flux motion in a Josephson-coupled layer model of high-Tc superconductors " *Phys. Rev.* **B42**, pp.6209–6216, 1990.
18. M.Tachiki, M.Machida, and T.Koyama "Josephson Vortex Flow States and Josephson Plasma Excitation in High Tc Superconductors", to be published in *Physica* **C**.
19. S.Sakai, P.Bodin, and N.F.Pedersen, "Fluxons in Thin-Film Superconductor-Insulator Superlattices", *J. Appl. Phys.* **73** (5), pp.2411–2418 1993.
20. M.Machida, T.Koyama, and M.Tachiki, " Dynamics of Josephson Vortices Interacting with Josephson Plasma Waves and Related Electromagnetic Behaviors", (in preparation).